

10-1-2004

Development of a microwave calorimeter for simultaneous thermal analysis,

Alan Nesbitt

Manchester Materials Science Centre, UMIST

P Navabpour

Manchester Materials Science Centre, UMIST

B Degamber

Royal Military College of Science, Cranfield University

C Nightingale


Thermal Instruments

G Fernando

Royal Military College of Science, Cranfield University

See next page for additional authors

Follow this and additional works at: http://epubs.glyndwr.ac.uk/aer_eng

 Part of the [Analytical Chemistry Commons](#), [Condensed Matter Physics Commons](#), [Engineering Science and Materials Commons](#), [Heat Transfer, Combustion Commons](#), [Materials Chemistry Commons](#), [Organic Chemistry Commons](#), [Physical Chemistry Commons](#), [Polymer and Organic Materials Commons](#), [Polymer Chemistry Commons](#), [Polymer Science Commons](#), [Process Control and Systems Commons](#), and the [Structures and Materials Commons](#)

Recommended Citation

Nesbitt, A., Navabpour, P., Degamber, P. Nightingale, C. Mann, T., Fernando, G. and Day R.J. (2004) 'Development of a microwave calorimeter for simultaneous thermal analysis, infrared spectroscopy and dielectric measurements', *Measurement Science and Technology* Vol. 15, No. 11, pp. 2313–2324

Development of a microwave calorimeter for simultaneous thermal analysis,

Abstract

An instrument has been developed for monitoring cure processes under microwave heating conditions. The main function of the instrument was a calorimeter for performing microwave thermal analysis. A single model resonant cavity was used as the heating cell in the microwave calorimeter.

Thermal analysis measurements were obtained by monitoring the variation in the microwave power that was required to maintain controlled heating of the sample. The microwave thermal analysis data were analogous to conventional differential scanning calorimetry measurements. The dielectric properties of the sample, as a function of the extent of cure, have been obtained using perturbation theory from the changes in resonant frequency and quality factor of the microwave cavity during heating. Additionally, remote sensing fibre-optic probes have been employed to measure real time *in situ* infrared spectra of the sample during the cure reaction. In this paper, we describe the design and operation of the microwave calorimeter. Examples of experimental results are also presented.

Keywords

microwave, calorimeter, calorimetry, dielectric properties, infrared spectroscopy, thermal analysis

Disciplines

Aerospace Engineering | Analytical Chemistry | Chemical Engineering | Chemistry | Condensed Matter Physics | Engineering | Engineering Science and Materials | Heat Transfer, Combustion | Materials Chemistry | Organic Chemistry | Physical Chemistry | Physics | Polymer and Organic Materials | Polymer Chemistry | Polymer Science | Process Control and Systems | Structures and Materials

Comments

Copyright © Institute Of Physics 2004. This is the authors final version and the full published version is available at <http://dx.doi.org/10.1088/0957-0233/15/11/018> and via the publishers link at <http://iopscience.iop.org/0957-0233/15/11/018>

Authors

Alan Nesbitt, P Navabpour, B Degamber, C Nightingale, G Fernando, and Richard Day

Development of a Microwave Calorimeter for Simultaneous Thermal Analysis, Infrared Spectroscopy and Dielectric Measurements

A. Nesbitt¹, P. Navabpour¹, B. Degamber², C. Nightingale¹, T. Mann³, G. Fernando², R.J. Day¹

¹Manchester Materials Science Centre, Grosvenor Street, Manchester, M1 7HS

²Royal Military College of Science, Cranfield University, Swindon, Wiltshire, SN6 8LA

³Thermal Instruments, PO Box 188, Beaconsfield, Buckinghamshire, HP9 2GB

Abstract

An instrument has been developed for monitoring cure processes under microwave heating conditions. The main function of the instrument was a calorimeter for performing microwave thermal analysis. A single mode resonant cavity was used as the heating cell in the microwave calorimeter. Thermal analysis measurements were obtained by monitoring the variation in the microwave power that was required to maintain controlled heating of the sample. The microwave thermal analysis data were analogous to conventional differential scanning calorimetry measurements. The dielectric properties of the sample, as a function of the extent of cure, have been obtained using perturbation theory from the changes in resonant frequency and quality factor of the microwave cavity during heating. Additionally, remote sensing fibre optic probes have been employed to measure real time *in situ* infrared spectra of the sample during the cure reaction. In this paper, we describe the design and operation of the microwave calorimeter. Examples of experimental results are also presented.

Keywords: microwave, calorimeter, calorimetry, dielectric properties, infrared spectroscopy, thermal analysis

1. Introduction

The utilisation of microwave energy in heating applications has been mainly confined to the food, rubber, textile and wood industries. During the past few decades, however, microwave heating has been evaluated for a wider range of materials processing applications. In particular, microwave processing of ceramics has been extensively investigated in both academic and industrial scale research. In contrast, microwave

processing of polymers and polymer composites has received less attention in industry, due to poor process control and a lack of understanding of the curing mechanisms. Comparative studies of microwave and conventional thermal processing of polymeric materials have generated considerable debate regarding reported differences in reaction kinetics and mechanisms (see for example the review papers [1-3] and references therein). Several investigations have reported reaction rate enhancement, reduced gelation and vitrification times, different reaction temperature ranges and different reaction mechanisms for microwave curing compared with thermal curing [4-15]. Opposing studies have observed no difference in reaction kinetics for microwave and thermal processing of a range of polymer systems and have proposed that reaction pathway is independent of processing technique [16-23].

Comparative studies of cure reactions using thermal and microwave heating have been hindered by a number of factors. Firstly, comparable experimental techniques have not always been employed, therefore, it has been difficult to eliminate effects due to the techniques used. Secondly, reactions were not always followed *in situ*, but rather samples were removed from processing equipment and analysed separately. Common methods for characterisation of polymeric materials include thermal analysis techniques (differential scanning calorimetry (DSC); thermomechanical analysis (TMA); thermogravimetric analysis (TGA)) and Fourier Transform infrared (FTIR) spectroscopy. Conventional thermal analysis and FTIR equipment, however, can not be used to directly investigate microwave processing of polymers, since there is no method of applying heat to the samples using microwave energy. In most investigations of microwave curing of polymers, therefore, samples have been prepared using microwave processing equipment and have been subsequently analysed using conventional DSC [11-14,16-19], TMA [6,7] and FTIR [4,8-10,14,15,17] techniques. There have been a few studies in which equipment has been developed for following reactions *in situ*. These investigations include the use of remote sensing fibre optic systems for measurement of infrared spectra [5,20-25] and the monitoring of dielectric properties during cure [5,26-29]. In this paper we present the development of an instrument, which employs a range of *in situ* diagnostic techniques (thermal analysis; infrared spectroscopy; measurement of dielectric properties) for following cure reactions during microwave heating.

1.1 Microwave Thermal Analysis

Microwave heating of polymeric materials occurs as a result of dielectric polarisation, caused by the applied electric field, and the inability of this polarisation to follow the rapid changes in the electric field phase angle [1-3]. The time lag between the polarisation and electric field results in dissipation of electrical energy within the material as heat. The magnitude of this heating effect depends on the complex permittivity (ϵ^*) of the material;

$$\epsilon^* = (\epsilon' - j\epsilon'') \quad (1)$$

where ϵ' is the dielectric constant and ϵ'' is the dielectric loss factor. The dielectric constant is a measure of the polarisability of a material and indicates the capacity for storage of electrical energy as heat. The dielectric loss factor indicates the efficiency of conversion of electrical energy to thermal energy. At microwave frequencies, dielectric heating in polymeric materials occurs mainly as the result of two loss mechanisms. For polymers, the dielectric loss is mainly due to reorientation of permanent dipoles within the material. For polymer composites, in which particles or fibres are added to the polymer, there is an additional loss mechanism due to polarisation of interfacial charges (Maxwell-Wagner polarisation). The power dissipation in a material due to these loss mechanisms is proportional to the dielectric loss factor of the material. A dielectric heating equation relating power dissipation, applied electric field properties and dielectric properties of the material can be derived from Maxwell's equations [30];

$$P = 2\pi f \epsilon_0 \epsilon'' E^2 \quad (2)$$

where P is the power dissipation (Wm^{-3}), f is the electric field frequency (Hz), ϵ_0 is the permittivity of free space ($8.85 \times 10^{-12} \text{ Fm}^{-1}$), ϵ'' is the dielectric loss factor of the material and E is the average electric field strength (Vm^{-1}). Equation (2) assumes that the electric field is uniform throughout the material. The sample dimensions, therefore, should be sufficiently small that the effect of penetration depth, which is inversely proportional to the dielectric loss factor, is negligible. The dissipation of microwave power within the material results in an increase in the temperature of the material. The heating rate is given by the equation [30];

$$\frac{dT}{dt} = \frac{P}{\rho C_p} \quad (3)$$

where dT/dt is the heating rate ($^{\circ}\text{C s}^{-1}$), P is the power dissipation (W m^{-3}), ρ is the density of the material (g m^{-3}) and C_p is the specific heat capacity of the material ($\text{J g}^{-1}\text{C}^{-1}$).

We have performed microwave thermal analysis measurements by monitoring the microwave power as a function of sample temperature during controlled heating programs. The changes in enthalpy, associated with processes such as chemical reactions, phase changes, etc., were reflected by variation in the power required for maintaining a given heating program. During exothermic processes, less energy was required to maintain the sample temperature at the program set point and, therefore, a decrease in the power required for heating was observed. Similarly, during endothermic processes, more energy was required and, therefore, an increase in power was observed. The data obtained was analogous to conventional power compensated DSC measurements. The technique differs from conventional thermal analysis, however, because the changes in the dielectric loss factor, which are associated with chemical reactions and phase changes, will also have an effect on the power dissipation in the sample (equation (2)) and the subsequent heating rate (equation (3)).

Similar methods for microwave thermal analysis have been adopted by Parkes *et al* [31]. Thermal transitions associated with phase changes and decomposition processes in simple chemical systems (i.e. inorganic, organo-metallic and organic compounds) have been investigated [32,33]. The microwave equipment comprised of a variable power source and a rectangular waveguide applicator. A complex tuning method was used, in order to produce a standing wave in the applicator, with maximum electric field in the sample, and to maximise the power absorbed by the sample. The tuning method involved the variation of; (i) the length of the waveguide, using an internal short circuit; (ii) the lateral position of an iris within the waveguide; and (iii) a four stub tuner. Differential thermal analysis measurements were performed by monitoring the temperature difference between the sample and a ceramic sample cell. Shielded thermocouples were used for temperature measurement. The sample cell was microwave susceptible and, therefore, was heated by the applied electric field. The mass of the sample cell (~50 g) was much larger than the mass of the sample (0.1-0.4 g), therefore, it would be very difficult to differentiate between direct microwave heating of the sample and heat conduction from the sample cell.

The instrumentation design that we have adopted for microwave thermal analysis used a simple cylindrical resonant cavity as the heating cell. Samples were placed in the centre of the cavity in the region of maximum electric field. Fine adjustments were made to the microwave source frequency during heating to take account of changes in the cavity resonant frequency as the sample cured. Controlled heating was achieved by adjustment of the microwave source power. The sample temperature was monitored directly using a microwave transparent sensor. Glass sample tubes (~5 g) were used with sample masses in the range 0.3-0.4 g.

1.2 Infrared Spectroscopy

Remote sensing systems have been developed for the measurement of infrared spectra during processing of polymer samples [5,20-25]. The detection systems used near-infrared transmitting optical fibres as the spectroscopic probes, which were remotely coupled to an infrared spectrometer.

Marand *et al* [5] have measured attenuated total reflection (ATR) spectra, using a single unsheathed optical fibre embedded in the sample. In this technique, infrared light passed along the fibre in a series of total internal reflections. At each internal reflection, an evanescent wave extended beyond the surface of the fibre and interacted with the sample. The light passing through the fibre was attenuated at wavelengths where the sample absorbed energy and a spectrum was obtained. A limitation of this technique was that the penetration depth was very small (typically ~1 μm) and therefore the ATR infrared spectra may not be representative of curing processes occurring in the bulk of the sample.

Alternative detection systems have been developed for measuring transmission spectra during cure [20-24]. In transmission spectroscopy, infrared light passed from a source, through the sample and was collected by a detector. The limitation of a short optical path length associated with the ATR technique was therefore avoided. In the remote sensing systems, single unsheathed optical fibres were used as the source and collector probes. The fibres were embedded in the sample, with an optical path length of ~2 mm through the sample.

The main disadvantage of the remote sensing systems described above, in which single fibre spectroscopic probes were used, was the low signal to noise ratio due to the limited

throughput of light. In addition, in this technique as well, the size of the sample monitored (cylinder of 200 μm diameter and 2 mm length) was small in comparison to the actual sample size. The signal to noise ratio can be improved by using multi-fibre spectroscopic probes. A remote sensing system for performing diffuse reflectance spectroscopy, which used a multi-fibre non-contact probe, has been developed at Cranfield University [25]. The probe consisted of a bundle of optical fibres, which was bifurcated at one end into groups of source and collector fibres. The active end of the probe consisted of a random arrangement of source and collector fibres, which were polished, in order to maximise the throughput of light. Samples were cured on glass or alumina plates in a commercial microwave oven. Reflectance spectra were measured with the probe positioned 1 mm above the sample surface. Infrared light passed from the source fibres, through the sample and was reflected from the glass or alumina plates. The reflected light passed through the sample, into the collector fibres and was detected by the spectrometer. The overall optical path length through the sample was ~ 4 mm.

We have modified the experimental arrangement used by Degamber and Fernando [25], in order to measure transmission near-infrared spectra during microwave heating. Samples were cured in glass tubes in a cylindrical resonant cavity. Two separate multi-fibre non-contact probes were used for the infrared source and collector.

1.3 Measurement of Dielectric Properties

Using cavity perturbation theory, the dielectric properties of low loss ($\epsilon'' < 3$) materials can be calculated from the changes in resonant frequency and quality factor of a resonant cavity following insertion of a sample [34]. The theory assumes that the changes in the electromagnetic field and the stored energy are small. The assumptions are valid if the unperturbed quality factor is large and the frequency shift is much smaller than the resonant frequency. The former is dependent on the design and construction of the cavity and the selected resonant mode, while the latter can be achieved if the sample volume is much smaller than the volume of the cavity. The dielectric properties can be calculated using the equations;

$$(\epsilon' - 1) = A \frac{(f_c - f_s)}{f_c} \frac{V_c}{V_s} \quad (4)$$

$$\varepsilon'' = B \left(\frac{1}{Q_s} - \frac{1}{Q_c} \right) \frac{V_c}{V_s} \quad (5)$$

where ε' is the dielectric constant, ε'' is the dielectric loss factor, f_c and f_s are the unperturbed and perturbed resonant frequencies, respectively, Q_c and Q_s are the unperturbed and perturbed unloaded quality factors, respectively, and V_c and V_s are the volumes of the cavity and sample, respectively. The parameters A and B are independent of the dielectric properties of the sample material and dependent on the cavity and sample geometries and the resonant mode. The values of A and B can be determined analytically only for a few specific configurations of cavity, sample and resonant mode. In other cases, the values of A and B can be determined experimentally by calibration using materials with known dielectric properties.

The quality factor (Q) of a resonant cavity is a measure of the ratio of the stored energy to the power loss within the cavity [35];

$$Q = 2\pi f \frac{\text{average stored energy}}{\text{power loss}} \quad (6)$$

where f is the resonant frequency of the cavity. The parameters Q_s and Q_c in equation (5) are unloaded quality factors, which represent the losses in the isolated cavity with and without a sample, respectively. Experimentally, the cavity is not isolated, but rather it is physically connected to an external circuit. The quality factor for the entire system is known as the loaded quality factor (Q_L) and it can be divided into terms, which represent the losses in the individual elements of the system [35];

$$\frac{1}{Q_L} = \frac{1}{Q} + \frac{1}{Q_E} \quad (7)$$

where Q is the unloaded quality factor, which represents losses in the resonant cavity and dielectric sample (if present) and Q_E is the external quality factor, which represents losses in the external circuit. Usually, the external circuit is connected to the cavity using a simple coupling device (e.g. a coupling aperture between a waveguide transmission line and the cavity or a coupling antenna between a coaxial line and the cavity). The efficiency of coupling between the external circuit and resonant cavity can be measured as a coupling

coefficient (β), which is defined as the ratio of the unloaded quality factor to the external quality factor [35];

$$\beta = \frac{Q}{Q_E} \quad (8)$$

The loaded quality factor can be measured directly and the unloaded quality factor can then be determined from the measured value of Q_L if the coupling coefficient β is known;

$$Q = (1 + \beta)Q_L \quad (9)$$

Perturbation techniques have previously been successfully employed to monitor the dielectric properties of polymers during microwave heating [5,26-29]. We have measured changes in dielectric properties during cure using a cylindrical resonant cavity. The dielectric constant and loss factor were calculated using equations (4) and (5) with the parameters A and B determined by calibration. The resonant frequency and the loaded quality factor were measured during heating from the frequency response of the cavity. The unloaded quality factor was calculated using equation (9).

2. Instrumentation

An instrument has been developed for monitoring cure reactions during microwave heating. The main function of the instrument was a microwave heated calorimeter. The instrumentation for the calorimeter has been developed at UMIST. A remote sensing fibre optic system for measurement of *in situ* near-infrared spectra has been developed at Cranfield University. A schematic of the instrumentation is shown in Figure 1, with the components grouped according to function; (i) calorimeter heating cell; (ii) microwave components, which included a variable frequency power source and power sensors; (iii) temperature measurement and PID control system; (iv) infrared spectrometer, with remote sensing fibre optic probes; and (v) process control and data acquisition.

2.1 Calorimeter Heating Cell

A single mode resonant cavity was used as the heating cell of the calorimeter. A cylindrical cavity operating in the TE_{111} mode with a resonant frequency of 2.45 GHz was selected.

The required dimensions for the cavity (radius 58 mm; height 77 mm) were determined using analytical methods [35]. The geometry of the cavity was verified using numerical simulation (Ansoft; High Frequency Structure Simulator (HFSS v.8.5)). The simulated electric field distribution for the TE₁₁₁ mode in a model cavity is shown in Figure 2. The E field vectors were perpendicular to the cavity axis with the maximum electric field magnitude at the centre of the cavity.

The single mode microwave cavity has been constructed from a section of brass tube with two brass end plates. The cylindrical section of the cavity was constructed with knife-edge seals for the end plates, in order to improve the electrical contact. The microwave cavity had two 12.5 mm diameter holes in the centre of the end plates, which allowed access for a sample tube, the temperature sensor and the infrared probes. The dimension and position of these holes were chosen to ensure that there was no microwave leakage from the cavity. Additionally, the presence of the access holes did not perturb the resonant TE₁₁₁ mode (Figure 2). Sample tubes were inserted through the hole in the top of the cavity, such that the samples were located at the centre of the cavity (i.e. at the maximum in the electric field distribution).

The calorimeter has been used in two modes of operation; (i) simultaneous thermal analysis and dielectric measurements; and (ii) simultaneous thermal analysis and infrared spectroscopy. The arrangements of the sample tubes and probes within the cavity for these modes of operation are shown schematically in Figure 3. For simultaneous thermal analysis and dielectric measurements, 10 mm diameter test tubes were used. The sample tube was held in place with a PTFE support on the top of the cavity and the temperature sensor was inserted in the sample (Figure 3(a)). The measurement of infrared spectra required larger sample tubes to allow access for both temperature and infrared probes. For simultaneous thermal analysis and infrared spectroscopy, therefore, ~12 mm diameter sample tubes were used. In this case, flat bottom tubes were used, in order to maximise the throughput of light. The sample tube was supported by a PTFE holder for one of the infrared probes, which was inserted through the access hole in the bottom of the cavity (Figure 3(b)). The second infrared probe and temperature sensor were inserted into the sample tube. The mass of both types of sample tube was ~5 g. Sample masses in the range 0.3-0.4 g were used.

The resonant cavity was coupled with the microwave signal using three internal loop antennae. The loop antennae were located in the central plane of the cavity. A cross-sectional diagram of the cavity, which displays the relative positions of the antennae, is shown in Figure 4. The input antenna was constructed with a circumference equal to $\sim\lambda/2$ at the resonant frequency of 2.45 GHz ($\lambda/2\sim 61$ mm; diameter ~ 19.5 mm). This ensured close to critical coupling ($\beta\sim 1$) of the cavity with the external circuit and efficient transfer of power to the sample. The plane of this loop was oriented perpendicular to the cavity axis to ensure that the TE_{111} mode was excited. The microwave transmission signal was monitored using two undercoupled ($\beta\ll 1$) antennae. The internal antennae were connected to external coaxial connectors via sections of semi-rigid coaxial cable (RG402). The resonant cavity was connected to the microwave hardware via flexible 50Ω coaxial cables.

2.2 Microwave Components

The calorimeter power source consisted of a narrow band (2.3-2.7 GHz) solid state amplifier (Microwave Amplifiers Ltd.), which was driven by the RF output of a network analyser (Hewlett Packard; Model HP8714ET). The network analyser output power had a maximum value of 0 dBm (1 mW) and a resolution of 0.01 dB (0.23%). The gain of the amplifier was 44.5dB. The maximum source power for this configuration was ~ 30 W. An internal isolator in the solid state amplifier protected the amplifier and network analyser against power reflected from the cavity.

The output from the microwave amplifier was fed via a directional coupler to the cavity. The directional coupler allowed the signal reflected from the cavity to be monitored. The reflection and transmission signals were attenuated before detection, in order to protect the microwave sensors. The reflection and transmission powers were measured using power sensors (Anritsu; Model MA2472B) connected to a power meter (Anritsu; Model ML2438A). The attenuated (-30 dB) transmission signal was also monitored by the network analyser to allow the determination of dielectric properties during heating.

2.3 Temperature Measurement and Control System

The temperature control system for the calorimeter used a feedback loop between the source power and the sample temperature. The control system consisted of a microwave transparent temperature sensor and a commercially available PID process controller. The

sample temperature was measured using a fluoroptic probe and thermometer (Luxtron Corporation; SFF immersion probe; Model 790 thermometer). The fluoroptic probe was comprised of a 200 μm all-silica fibre with a temperature sensitive phosphor tip and Teflon coating. The operating temperature of the probe was -25°C to $+300^{\circ}\text{C}$. The temperature probe was protected using a thin wall capillary tube (ID 1.5 mm) and placed inside the sample (Figure 3). The temperature was monitored at a sampling rate of 4 Hz and with an accuracy of $\pm 1^{\circ}\text{C}$. A programmable PID process controller (CAL Controls Ltd.; Model CAL9500P) was used to control the sample temperature. The PID control parameters were optimised using an in-built auto-tune facility. The controller supported heating programs with multiple stages (temperature ramp (heating or cooling); isothermal dwell; temperature step). The heating programs were stored in the internal memory of the controller.

Controlled heating has been achieved for ramp rates in the range $2\text{--}15^{\circ}\text{Cmin}^{-1}$ and isothermal temperatures in the range $90\text{--}190^{\circ}\text{C}$. Typical temperature profiles for heating epoxy resin samples are shown in Figure 5. The temperature ramps were reasonably linear, with only a slight oscillation about the heating program set point ramp (Figure 5(a)). For a heating rate of $2^{\circ}\text{Cmin}^{-1}$, the sample temperature was within $\pm 0.25^{\circ}\text{C}$ of the program set point temperature, while for a heating rate of $15^{\circ}\text{Cmin}^{-1}$, the sample temperature was within $\pm 0.5^{\circ}\text{C}$ of the program set point temperature. For isothermal heating programs, the sample temperature was increased to the set point at a high heating rate ($\sim 150^{\circ}\text{Cmin}^{-1}$), with minimal overshoot and was reasonably stable at the set point (Figure 5(b)). For a set point of 110°C , the sample temperature varied by $\pm 0.4^{\circ}\text{C}$, with an average value of 110.5°C , while for a set point of 190°C , the sample temperature varied by $\pm 0.5^{\circ}\text{C}$, with an average value of 190.9°C .

2.4 Infrared Spectrometer and Remote Sensing Probes

Infrared spectra were recorded using a FTIR spectrometer (Nicolet Nexus), which was set to operate in the near-infrared spectral region ($4000\text{--}11000\text{ cm}^{-1}$). The spectrometer was fitted with two sub-miniature (SMA) fibre optic ports for the light source and the detector. The remote sensing probes consisted of bundles of 20 optical fibres and were attached to the spectrometer via the SMA fibre optic ports. Silica-silica low hydroxyl content optical fibres (Bfi Optilas) were used. The fibres were comprised of a 200 μm core and 220 μm cladding, with a 250 μm PYROCOATTM coating. The operating temperature of the fibres was -65°C to $+300^{\circ}\text{C}$. The source probe fibres were held together in a PTFE tube with an

outside diameter of 5 mm. The collector probe fibres were held together in a glass tube with an outside diameter of 6 mm. The active ends of the infrared probes were polished to ensure maximum throughput of light.

A schematic diagram showing the arrangement of the remote sensing infrared transmission probes in the microwave cavity is shown in Figure 3(b). The collector probe was inserted through the hole in the bottom of the cavity and was held in place with a PTFE support. Flat bottom sample tubes were inserted through the hole in the top of the cavity and were supported by the PTFE holder for the infrared collector probe. The infrared source probe was inserted into the sample tube and was positioned above the surface of the sample. The optical path length through the sample was ~4 mm.

2.5 Process Control and Data Acquisition

Process control and data acquisition for thermal analysis and dielectric measurements were performed using software developed at UMIST. The program code was written in Visual C++ (Microsoft Visual C++ 6.0) using Standard Instrument Control Library (HP SICL) commands to control the I/O interfaces between the computer and the calorimeter hardware. The network analyser and microwave power meter were controlled via general purpose interface bus (GPIB) connections. The fluoroptic thermometer was controlled via a serial communications (RS232) connection. The fluoroptic thermometer provided an analog output voltage (0-5 V; resolution 2.5 mV), proportional to the sample temperature, which was input to the process controller. The process controller produced an analog output voltage (0-5 V; resolution 5 mV), proportional to the required source power, which was input to the computer via a single channel 12-bit analog-digital converter (Pico Technology Ltd.; Model ADC-12).

The software performed a loop of operations (Figure 6), which maintained controlled heating and recorded data. The transmission signal was monitored by the network analyser periodically during heating. The resonant frequency and quality factor were measured from the transmission signal peak position and bandwidth. The computer set the network analyser to CW mode at the resonant frequency of the cavity and varied the network analyser output power to control heating. The sample temperature was measured by the fluoroptic thermometer and recorded by the computer. The thermometer analog voltage was input to the process controller. The process controller generated a control voltage,

which was proportional to the source power required to maintain the heating program. The computer read the control voltage and set the required network analyser output power. The reflection and transmission powers were recorded by the computer. The power required for heating the sample was calculated by subtraction of the reflection and transmission powers from the source power. The data was saved and the control cycle repeated until the end of the heating program. The process control cycle time was 0.25 s and was limited by the sampling rate of the thermometer. The microwave source power was updated every cycle. The resonant frequency and quality factor were measured at a user defined period.

Infrared spectra were acquired using a separate control system developed at Cranfield University. A macro program (Nicolet) was used to control the FTIR spectrometer and collect data continuously during microwave heating. The spectrometer was set to scan the near-infrared spectral region ($4000\text{-}11000\text{ cm}^{-1}$) with a resolution of 8 cm^{-1} . The near-infrared spectra were recorded every 30 s as a co-addition of 48 scans.

3. *Experimental Measurements and Data Analysis*

The microwave calorimeter has been used for thermal analysis, infrared spectroscopy and the measurement of dielectric properties during microwave heating. The infrared probes used in the spectroscopic measurements caused the resonant cavity to become highly perturbed, resulting in a large decrease in the quality factor of the cavity. Measurements of dielectric properties, therefore, could not be made at the same time as the measurement of infrared spectra. As a result of this, the calorimeter has been used in two separate modes of operation; (i) microwave thermal analysis, with simultaneous *in-situ* infrared spectroscopy; and (ii) microwave thermal analysis, with simultaneous measurement of dielectric properties.

The most commonly researched of the thermosetting polymers are the epoxy resin systems. We have studied the cure reactions for a range of epoxy resin systems using the microwave calorimeter. Comparative kinetic analysis for the reactions occurring under microwave and conventional thermal heating conditions has been performed. The results of these investigations are presented in detail elsewhere [36,37]. In this paper, a number of examples of experimental measurements have been selected, in order to illustrate the operation of the calorimeter. Typical measurements for two epoxy resin systems have been included. The first material was a three component resin system, which consisted of an

epoxy resin, an acid anhydride hardener (HY917; Vantico Ltd.) and an accelerator (DY073; Vantico Ltd.). The epoxy resin component was a liquid diglycidyl ether of bisphenol-A (DEGBA) with average molecular weight 384 g mol^{-1} and epoxy value 5.2 equivalents per kg. The HY917 hardener component was 4-cyclohexene-1,2-dicarboxylic anhydride. The DY073 accelerator was an amine-phenol complex, which consisted of dibutyl phthalate, tributylamine and phenol. Samples were prepared by mixing the DEGBA, HY917 and DY073 components in a ratio of 1.0:0.85:0.02 by weight. The second material was a single component premixed polyfunctional epoxy resin and hardener (RTM6; Hexcel Composites).

3.1 Thermal Analysis

Thermal analysis data were obtained by measuring the power required for maintaining controlled heating programs, as a function of time and sample temperature. Signal noise in the raw data was removed by applying a Fast Fourier Transform filter. The thermal analysis data obtained from the microwave calorimeter have been compared to measurements made with a conventional differential scanning calorimeter (Perkin Elmer; Pyris 1 DSC). Material melting points were used as measurement standards, in order to ensure that the calibration of the sample temperature in the microwave calorimeter was correct. Measurements of the melting point of stearic acid using the microwave calorimeter and the conventional DSC are shown in Figure 7. Similar peak temperatures ($T_p \sim 69^\circ\text{C}$) and peak widths ($\Delta T \sim 3^\circ\text{C}$) were observed in both measurements.

Measurements of the reaction exotherm for curing the DEGBA-HY917-DY073 resin system using the microwave calorimeter and the conventional DSC are shown in Figure 8. The exotherm peaks occurred over similar temperature ranges, with peak temperatures of $T_p = 148^\circ\text{C}$ in the microwave calorimeter data and $T_p = 156^\circ\text{C}$ in the DSC measurement. The main difference in the appearance of the two measurements was the signal background. In the conventional DSC measurement, a small difference was observed in the background before and after the exotherm peak, due to changes in the specific heat capacity of the material during the cure reaction. In the microwave calorimeter data, however, a large change was observed in the background during heating. In addition to the changes in specific heat capacity, this is due to changes in the dielectric loss of the material with increasing sample temperature and extent of cure. The dielectric loss factor decreased as the sample cured, therefore, the power dissipation in the sample (equation (2))

decreased, which resulted in an increase in the microwave power required to maintain the heating rate.

Reaction rates for microwave and thermal curing of the DEGBA-HY917-DY073 resin system have been calculated from the calorimetry data shown in Figure 8. Background correction in the microwave calorimeter and DSC data was performed using the Bandara method [38]. The corrected data plotted against reaction time was integrated to give the partial reaction enthalpy (proportional to the extent of cure) as a function of time. The fractional conversion (α) was calculated as the ratio;

$$\alpha = \frac{\Delta H_t}{\Delta H_R} \quad (10)$$

where ΔH_t is the partial reaction enthalpy at time t and ΔH_R is the total reaction enthalpy. Reaction rates were then determined by differentiation of the fractional conversion versus reaction time curves.

Fractional conversion and reaction rate, as a function of sample temperature, for microwave and thermal curing of the DEGBA-HY917-DY073 resin system are shown in Figure 9. The microwave and thermal reactions occurred over approximately the same temperature range. At low temperatures ($<150^\circ\text{C}$), a slight enhancement in reaction rate was observed for microwave curing, whereas at higher temperatures ($>150^\circ\text{C}$), the reaction rate for thermal curing was higher than for microwave curing. Additionally, the reaction rate peak for the microwave calorimeter data was asymmetric. This could be attributed to competing reaction pathways, with different but overlapping temperature ranges, which contribute to the measured reaction rate.

3.2 Infrared Spectra

Transmission near-infrared spectra have been recorded *in situ* during microwave heating using a FTIR spectrometer and remote sensing fibre optic probes. Infrared spectra recorded during the microwave cure reaction of the RTM6 resin system are shown in Figure 10. Well defined peaks were observed at $\sim 6600\text{ cm}^{-1}$ and $\sim 7000\text{ cm}^{-1}$, which have been attributed to the vibration of amine and hydroxyl groups, respectively. A small peak was observed at $\sim 4500\text{ cm}^{-1}$, which has been attributed to the vibration of epoxy groups. As the

cure reaction proceeded, the intensity of the epoxy and amine peaks decreased, due to reaction between epoxy and amine groups, while the intensity of the hydroxyl peak increased, due to formation of hydroxyl groups.

Reaction rates for microwave curing of the RTM6 resin system have been calculated from changes in the infrared peak areas with reaction time. The epoxy peak was small and poorly resolved, therefore, it has not been used in the analysis of the infrared spectra. The peak areas were normalised against the area of a reference peak. The peak at $\sim 5600\text{ cm}^{-1}$, which has been attributed to vibration of unreactive hydrocarbon groups, was selected as the reference peak. The fractional conversion (α) was calculated using the equation;

$$\alpha = 1 - \frac{A_t}{A_0} \quad (11)$$

where A_t is the normalised amine peak area at time t and A_0 is the normalised amine peak area at time $t = 0$. Reaction rates were then determined by differentiation of the fractional conversion versus reaction time curve. Fractional conversion and reaction rate, as a function of reaction time, for microwave curing of the RTM6 resin system are shown in Figure 11.

3.3 Dielectric Measurements

Changes in the dielectric properties of the epoxy resins during cure have been determined using cavity perturbation theory. The dielectric constant and loss factor were calculated using equations (4) and (5), respectively. The resonant frequency (f) was measured as the peak in the transmission signal and the loaded quality factor (Q_L) was determined from the transmission bandwidth;

$$Q_L = \frac{f}{\Delta f} \quad (12)$$

where Δf is the bandwidth 3 dB below the transmission peak. The unloaded quality factor (Q) was calculated using equation (9) assuming a coupling coefficient of $\beta \sim 1$. The unperturbed values f_c and Q_c were measured with an empty sample tube, a temperature probe and a capillary tube inside the resonant cavity. The perturbed values f_s and Q_s were

measured periodically as the sample was cured. The parameters A and B in equations (4) and (5) have been determined by calibration. The calibration was performed using measurements of dielectric properties obtained using a coaxial probe (Hewlett Packard; Model HP85070B).

The validity of using cavity perturbation theory to determine the dielectric properties depends on the magnitude of the quality factor of the resonant cavity and the relative shift in the resonant frequency when the cavity is perturbed. The unperturbed quality factor of the cavity was ~ 7000 , while the resonant frequency shift was ~ 2 MHz ($< 0.1\%$), therefore, reasonably accurate values of the dielectric properties were obtained using equations (4) and (5). The accuracy of the dielectric loss factor, however, also depends on the coupling coefficient. The microwave cavity has been designed to produce close to critical coupling ($\beta \sim 1$) between the cavity and the external circuit. The exact value of the coupling coefficient, however, depended on the sample material and size. Additionally, the coupling coefficient changed as the sample cured. Precise determination of the dielectric loss factor, therefore, would require measurement of the coupling coefficient during cure, which is not possible with the current instrumentation. In the data analysis outlined above, therefore, a constant value of $\beta = 1$ for the coupling coefficient during cure has been assumed.

The dielectric constant and loss factor, as a function of reaction time and fractional conversion, for microwave curing of the DEGBA-HY917-DY073 resin system are shown in Figure 12. The experimental data for the dielectric loss factor showed a significant scatter ($\sim 10\%$), however, the expected trends in the dielectric properties were observed. The dielectric constant and loss factor decreased with extent of cure, due to a depletion of the functional polar groups and a decrease in molecular mobility.

4.0 Conclusions

In this work a novel microwave calorimeter has been developed. This functions in a similar manner to a conventional differential scanning calorimeter. Comparison with a conventional DSC for a sample of steric acid showed, as expected, the melting behaviour measured using the two methods was very similar. The instrument has been used to assess the reaction kinetics of a number of epoxy resin systems and some examples are shown here. The new technique uses the cavity perturbation method to measure the dielectric properties of the sample concurrently with the thermal analysis.

It is also possible to obtain near infrared spectra at the same time as performing microwave thermal analysis. Thus chemical information about the nature of the reactions taking place can be obtained together with information regarding the kinetics of the reactions.

This new technique offers the prospect of being able to understand in detail the reactions that take place during microwave heating of materials and to be able to compare data with that of conventionally heated materials under the same controlled temperature program.

References

1. J. Jacob, L. H. L. Chia and F. Y. C. Boey, *Thermal and nonthermal interaction of microwave-radiation with materials*. Journal of Materials Science, **30**(21) (1995) 5321-5327.
2. J. B. Wei, T. Shidaker and M. C. Hawley, *Recent progress in microwave processing of polymers and composites*. Trends in Polymer Science, **4**(1) (1996) 18-24.
3. E. T. Thostenson and T. W. Chou, *Microwave processing: fundamentals and applications*. Composites Part A - Applied Science and Manufacturing, **30**(9) (1999) 1055-1071.
4. D. A. Lewis, J. D. Summers, T. C. Ward and J. E. McGrath, *Accelerated imidization reactions using microwave-radiation*. Journal of Polymer Science Part A - Polymer Chemistry, **30**(8) (1992) 1647-1653.
5. E. Marand, K. R. Baker and J. D. Graybeal, *Comparison of reaction-mechanisms of epoxy-resins undergoing thermal and microwave cure from in situ measurements of microwave dielectric-properties and infrared-spectroscopy*. Macromolecules, **25**(8) (1992) 2243-2252.
6. J. H. Wei, M. C. Hawley, J. D. Delong and M. Demeuse, *Comparison of microwave and thermal cure of epoxy-resins*. Polymer Engineering and Science, **33**(17) (1993) 1132-1140.
7. J. H. Wei, M. C. Hawley and M. T. Demeuse, *Kinetics modeling and time-temperature-transformation diagram of microwave and thermal cure of epoxy-resins*. Polymer Engineering and Science, **35**(6) (1995) 461-470.
8. J. Jacob, L. H. L. Chia and F. Y. C. Boey, *Comparative-study of methyl-methacrylate cure by microwave-radiation versus thermal-energy*. Polymer Testing, **14**(4) (1995) 343-354.

9. H. L. Chia, J. Jacob and F. Y. C. Boey, *The microwave radiation effect on the polymerization of styrene*. Journal of Polymer Science Part A - Polymer Chemistry, **34**(11) (1996) 2087-2094.
10. J. Jacob, L. H. L. Chia and F. Y. C. Boey, *Microwave polymerization of poly(methyl acrylate): Conversion studies at variable power*. Journal of Applied Polymer Science, **63**(6) (1997) 787-797.
11. F. Y. C. Boey, B. H. Yap and L. Chia, *Microwave curing of epoxy-amine system - effect of curing agent on the rate enhancement*. Polymer Testing, **18**(2) (1999) 93-109.
12. F. Y. C. Boey and S. K. Rath, *Microwave radiation curing of polymers: Using a temperature equivalent method for cure reaction analysis*. Advances in Polymer Technology, **19**(3) (2000) 194-202.
13. F. Y. C. Boey and B. H. Yap, *Microwave curing of an epoxy-amine system: effect of curing agent on the glass-transition temperature*. Polymer Testing, **20**(8) (2001) 837-845.
14. X. M. Fang, R. Hutcheon and D. A. Scola, *A study of the kinetics of the microwave cure of a phenylethynyl-terminated imide model compound and imide oligomer (PETI-5)*. Journal of Polymer Science Part A - Polymer Chemistry, **38**(14) (2000) 2526-2535.
15. R. V. Tanikella, S. A. B. Allen and P. A. Kohl, *Variable-frequency microwave curing of benzocyclobutene*. Journal of Applied Polymer Science, **83**(14) (2002) 3055-3067.
16. J. Mijovic and J. Wijaya, *Comparative calorimetric study of epoxy cure by Microwave vs thermal-energy*. Macromolecules, **23**(15) (1990) 3671-3674.
17. J. Mijovic, A. Fishbain and J. Wijaya, *Mechanistic modeling of epoxy amine kinetics. 2. Comparison of kinetics in thermal and microwave fields*. Macromolecules, **25**(2) (1992) 986-989.
18. C. Jordan, J. Galy, J. P. Pascault, C. More, M. Delmotte and H. Jullien, *Comparison of microwave and thermal cure of an epoxy-amine matrix*. Polymer Engineering and Science, **35**(3) (1995) 233-239.
19. C. Hedreul, J. Galy, J. Dupuy, M. Delmotte and C. More, *Kinetics modeling of a modified epoxy-amine formulation cured by thermal and microwave energy*. Journal of Applied Polymer Science, **68**(4) (1998) 543-552.
20. J. Mijovic, W. V. Corso, L. Nicolais and G. d'Ambrosio, *In situ real-time study of crosslinking kinetics in thermal and microwave fields*. Polymers for Advanced Technologies, **9**(4) (1998) 231-243.

21. D. G. Rogers, E. Marand, D. J. T. Hill and G. A. George, *Anomalies between microwave and thermal cure kinetics of epoxy-amine resin systems*. High Performance Polymers, **11**(1) (1999) 27-39.
22. D. J. T. Hill, G. A. George and D. G. Rogers, *A systematic study of the microwave and thermal cure kinetics of the TGDDM/DDS and TGDDM/DDM epoxy-amine resin systems*. Polymers for Advanced Technologies, **12**(3-4) (2001) 169-176.
23. D. J. T. Hill, G. A. George and D. G. Rogers, *A systematic study of the microwave and thermal cure kinetics of the DGEBA/DDS and DGEBA/DDM epoxy-amine resin systems*. Polymers for Advanced Technologies, **13**(5) (2002) 353-362.
24. D. G. Rogers, M. E. Bialkowski, D. J. T. Hill and G. A. George, *Kinetic study of epoxy-amine microwave cure reactions. Part I: design and operation of a single-mode resonant microwave cavity*. High Performance Polymers, **10**(4) (1998) 341-351.
25. B. Degamber and G. F. Fernando, *Fiber optic sensors for noncontact process monitoring in a microwave environment*. Journal of Applied Polymer Science, **89**(14) (2003) 3868-3873.
26. J. Jow, M. C. Hawley, M. Finzel, J. Asmussen, H. H. Lin and B. Manring, *Microwave processing and diagnosis of chemically reacting materials in a single-mode cavity applicator*. IEEE Transactions on Microwave Theory and Techniques, **35**(12) (1987) 1435-1443.
27. J. Jow, M. C. Hawley, M. Finzel and T. Kern, *Dielectric analysis of epoxy amine resins using microwave cavity technique*. Polymer Engineering and Science, **28**(22) (1988) 1450-1454.
28. J. Jow, M. C. Hawley, M. C. Finzel and J. Asmussen, *Microwave-heating and dielectric diagnosis technique in a single-mode resonant cavity*. Review of Scientific Instruments, **60**(1) (1989) 96-103.
29. M. C. Finzel, M. C. Hawley and J. Jow, *Dielectric-properties of a curing epoxy amine system at microwave-frequencies*. Polymer Engineering and Science, **31**(16) (1991) 1240-1244.
30. A. C. Metaxas and R. J. Meredith, *Industrial Microwave Heating*. 1993, London: Peter Peregrinus Ltd.
31. G. M. B. Parkes, G. Bond, P. A. Barnes and E. L. Charsley, *Development of a new instrument for performing microwave thermal analysis*. Review of Scientific Instruments, **71**(1) (2000) 168-175.

32. G. M. B. Parkes, P. A. Barnes, E. L. Charsley and G. Bond, *Microwave differential thermal analysis in the investigation of thermal transitions in materials*. Analytical Chemistry, **71**(22) (1999) 5026-5032.
33. G. M. B. Parkes, P. A. Barnes, G. Bond and E. L. Charsley, *Qualitative and quantitative aspects of microwave thermal analysis*. Thermochemica Acta, **356**(1-2) (2000) 85-96.
34. H. M. Altschuler, *Dielectric constant*, in *Handbook of Microwave Measurements*. 1963, Brooklyn Polytechnic Press: New York.
35. R. E. Collin, *Foundations for Microwave Engineering*. 1992, New York: McGraw-Hill.
36. P. Navabpour, A. Nesbitt, T. Mann and R. J. Day, *in preparation*.
37. P. Navabpour, A. Nesbitt, B. Degamber, T. Mann, G. F. Fernando and R. J. Day, *in preparation*.
38. U. Bandara, *A systematic solution to the problem of sample background correction in DSC curves*. Journal of Thermal Analysis, **31**(5) (1986) 1063-1071.

Figure Captions

Figure 1: Schematic of the instrumentation; (i) microwave calorimeter heating cell; (ii) microwave components (A: in-line attenuator; DC: directional coupler); (iii) temperature measurement and PID control system; (iv) remote sensing infrared spectrometer; and (v) process control and data acquisition (PC: personal computer; ADC: analog-digital converter; GPIB: general purpose interface bus; RS232: serial communications).

Figure 2: Simulated electric field distribution for the 2.45 GHz TE₁₁₁ mode in a model cavity; (a) relative magnitude of E field in three orthogonal planes; (b) E field vectors in the xy-plane; (c) E field vectors in the xz-plane.

Figure 3: Schematic cross-section (vertical plane) of microwave cavity showing arrangement of sample tube, temperature sensor and infrared probes; (a) thermal analysis and dielectric measurements; (1) sample tube; (2) temperature sensor and capillary tube; (3) PTFE support; (b) thermal analysis and infrared spectroscopy; (1) sample tube; (2) temperature sensor and capillary tube; (3) infrared source probe; (4) infrared collector probe; (5) PTFE support.

Figure 4: Schematic cross-section (horizontal plane) of microwave cavity showing arrangement of coupling antennae; (1) input antenna; (2) transmission antenna; (3) semi-rigid coaxial cable; (4) coaxial connector; (5) access hole in cavity end plate.

Figure 5: Typical temperature profiles for controlled heating of epoxy resin samples using the microwave calorimeter; (a) temperature ramps at heating rates 2°Cmin⁻¹ and 15°Cmin⁻¹ (RTM6 samples); (b) isothermal heating at set points 110°C and 190°C (DEGBA- HY917-DY073 and RTM6 samples, respectively).

Figure 6: Control and data acquisition loop performed by the process control software.

Figure 7: Endothermic peak for the melting point of stearic acid at a heating rate of 2°Cmin⁻¹; (a) microwave calorimeter measurement; (b) DSC measurement.

Figure 8: Reaction exotherm for the dynamic curing of an epoxy-acid anhydride resin (DEGBA-HY917-DY073) at a heating rate of $5^{\circ}\text{Cmin}^{-1}$; (a) microwave calorimeter measurement; (b) DSC measurement.

Figure 9: Fractional conversion (circles) and reaction rate (squares), as a function of sample temperature, for dynamic curing of an epoxy-acid anhydride resin (DEGBA-HY917-DY073) at a heating rate of $5^{\circ}\text{Cmin}^{-1}$; (a) microwave calorimeter data; (b) DSC data. Data calculated from calorimetry measurements (Figure 8).

Figure 10: *In situ* near-infrared spectra for isothermal (160°C) microwave curing of an epoxy-amine resin (RTM6), recorded at reaction times of 0, 15, 25, 27 and 60 min. The spectra show depletion of the amine peak ($\sim 6600\text{ cm}^{-1}$) and growth of the hydroxyl peak ($\sim 7000\text{ cm}^{-1}$) as the reaction proceeded.

Figure 11: Fractional conversion (circles) and reaction rate (squares), as a function of reaction time, for isothermal microwave curing of an epoxy-amine resin (RTM6) at 160°C . Data calculated from depletion of amine peak in near-infrared spectra (Figure 10).

Figure 12: Dielectric constant (squares) and dielectric loss factor (circles), as a function of (a) reaction time and (b) fractional conversion, for an epoxy-acid anhydride resin (DEGBA-HY917-DY073) cured at 110°C .

Fig. 1.

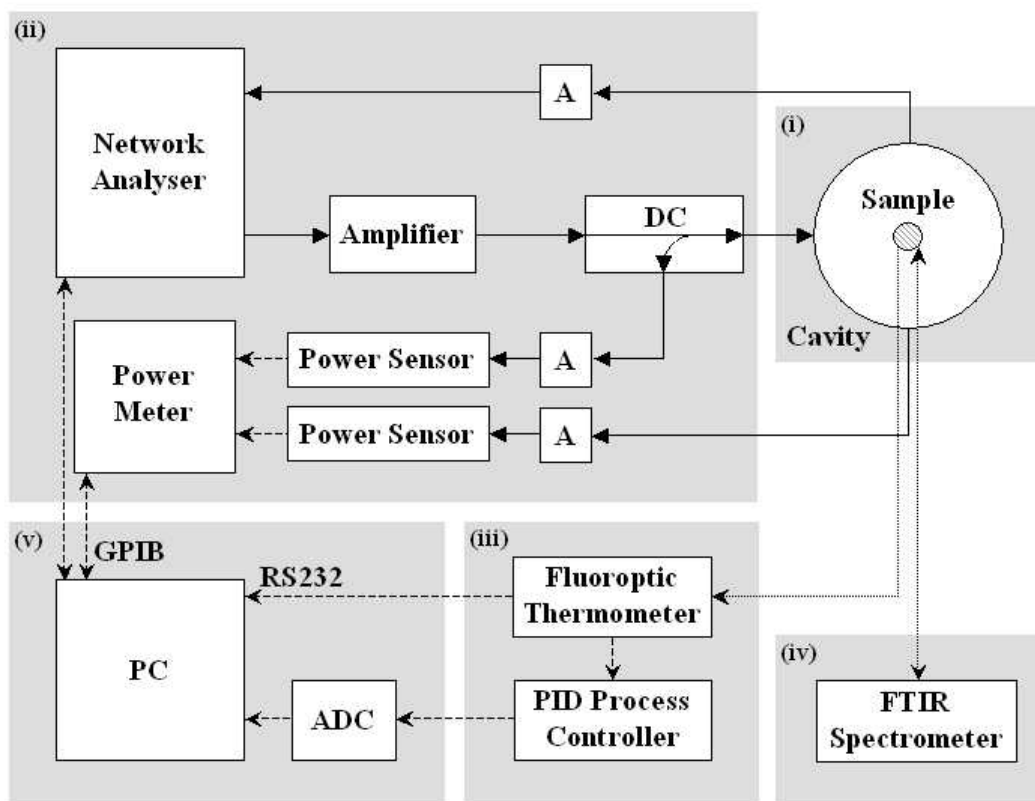


Fig. 2(a,b+c).

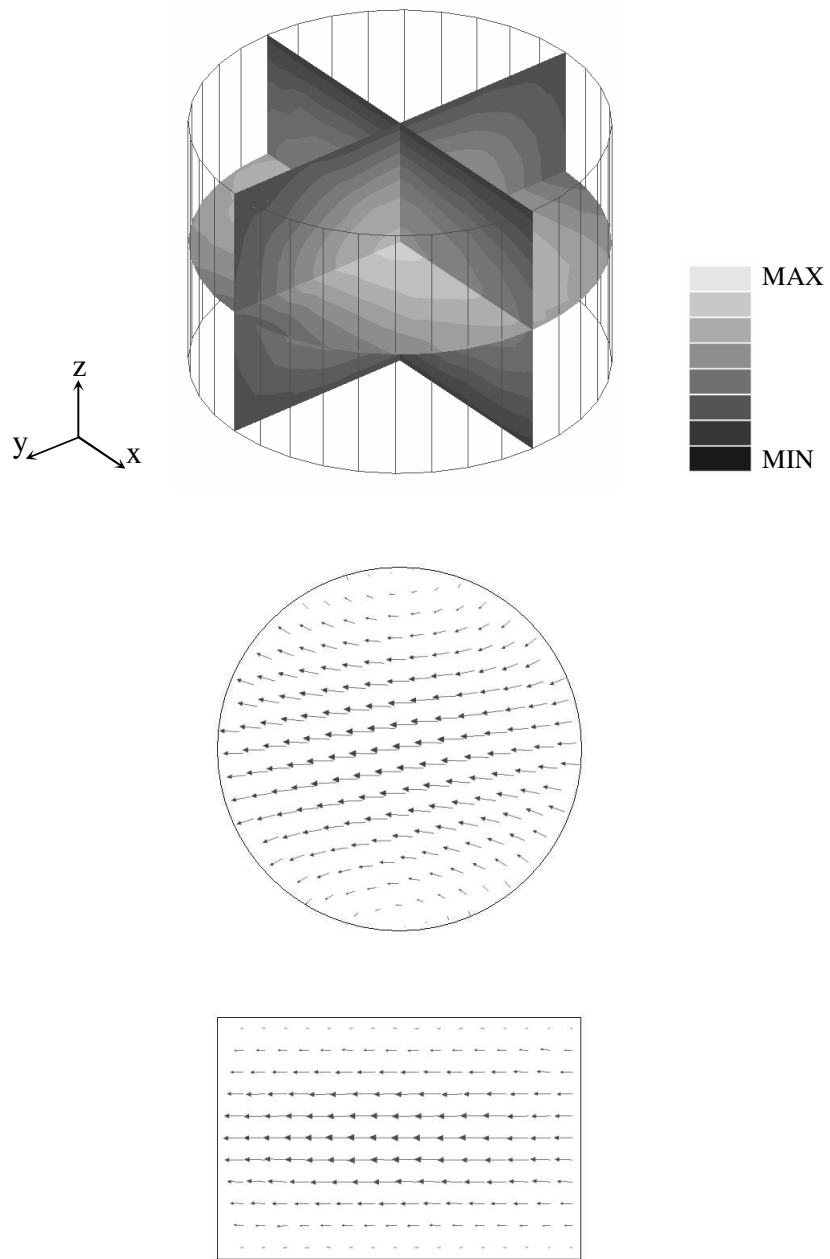


Fig. 3(a+b).

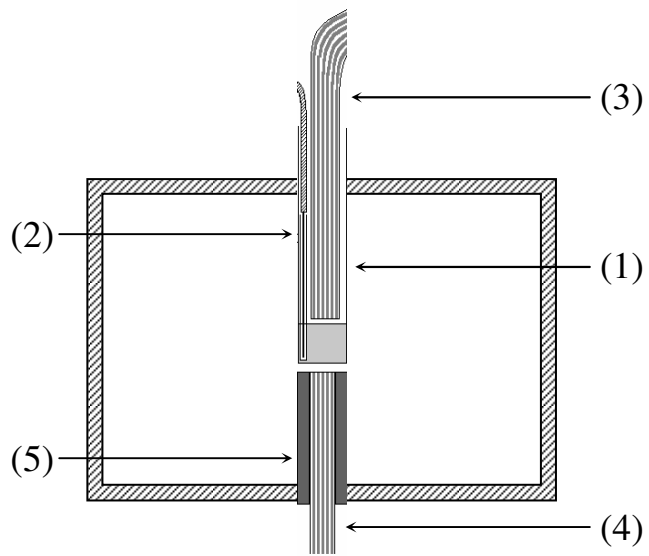
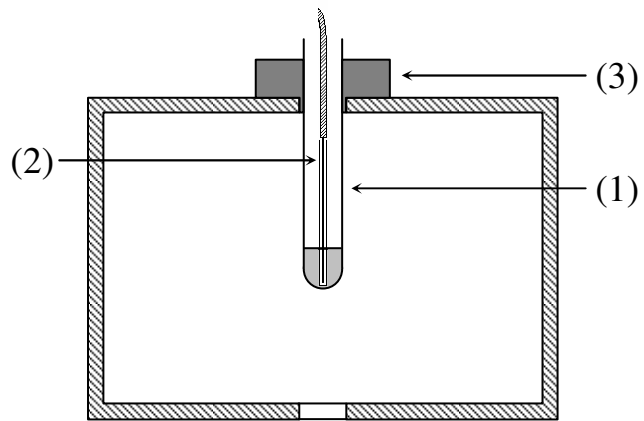


Fig. 4.

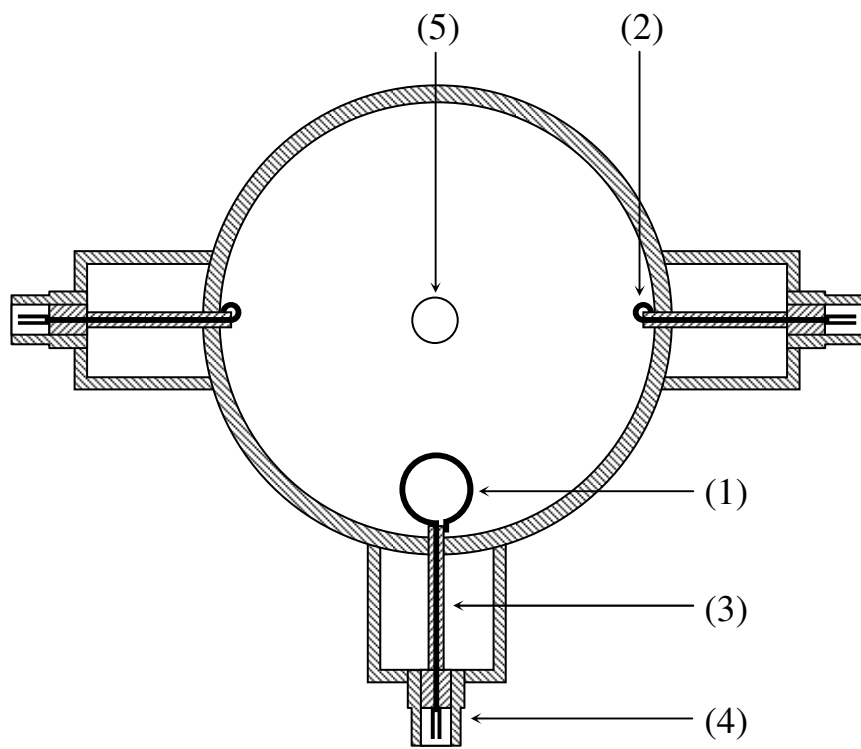


Fig. 5(a+b).

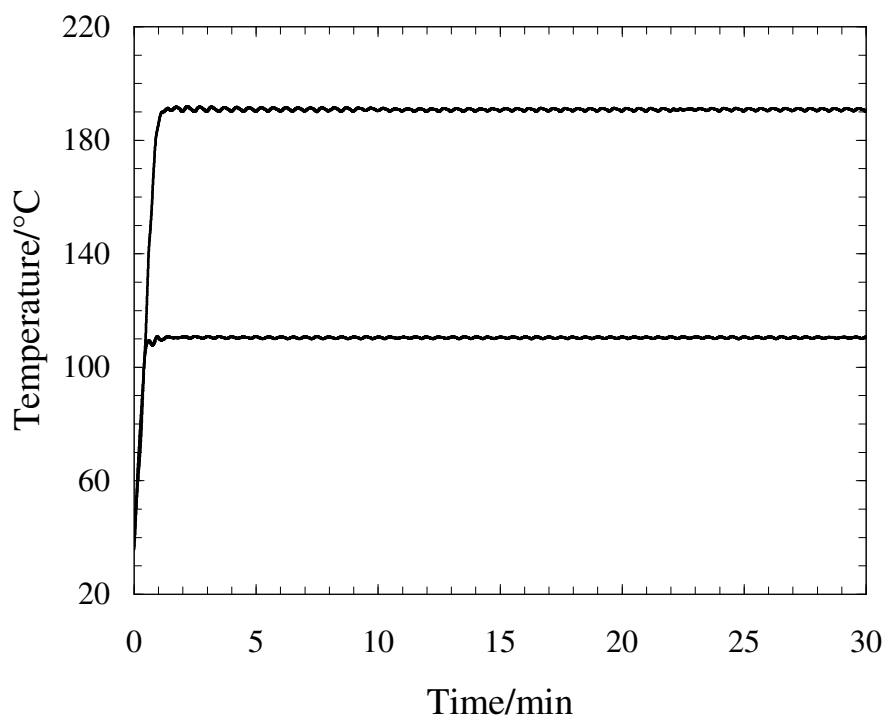
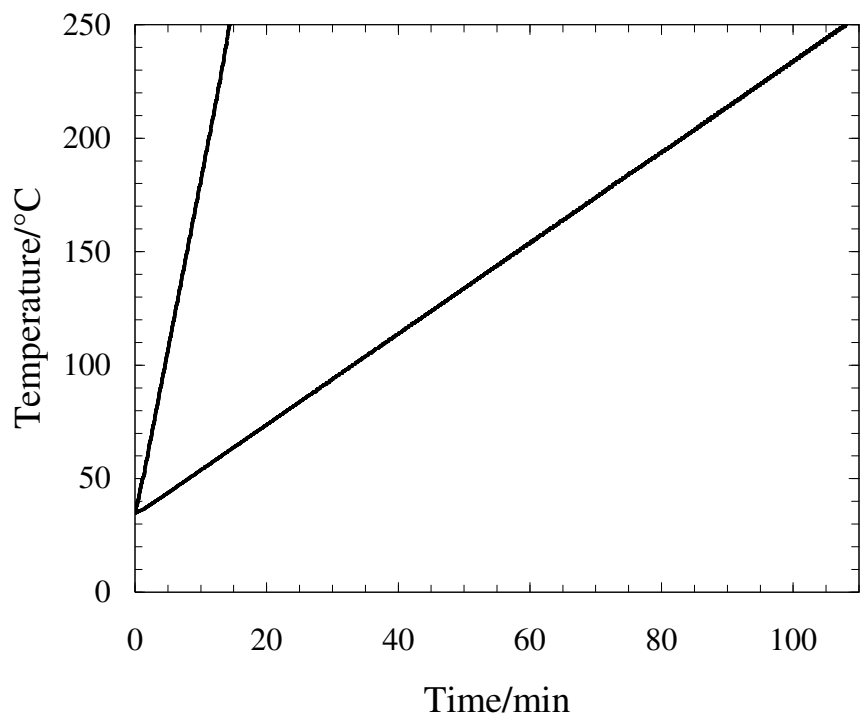


Fig. 6.

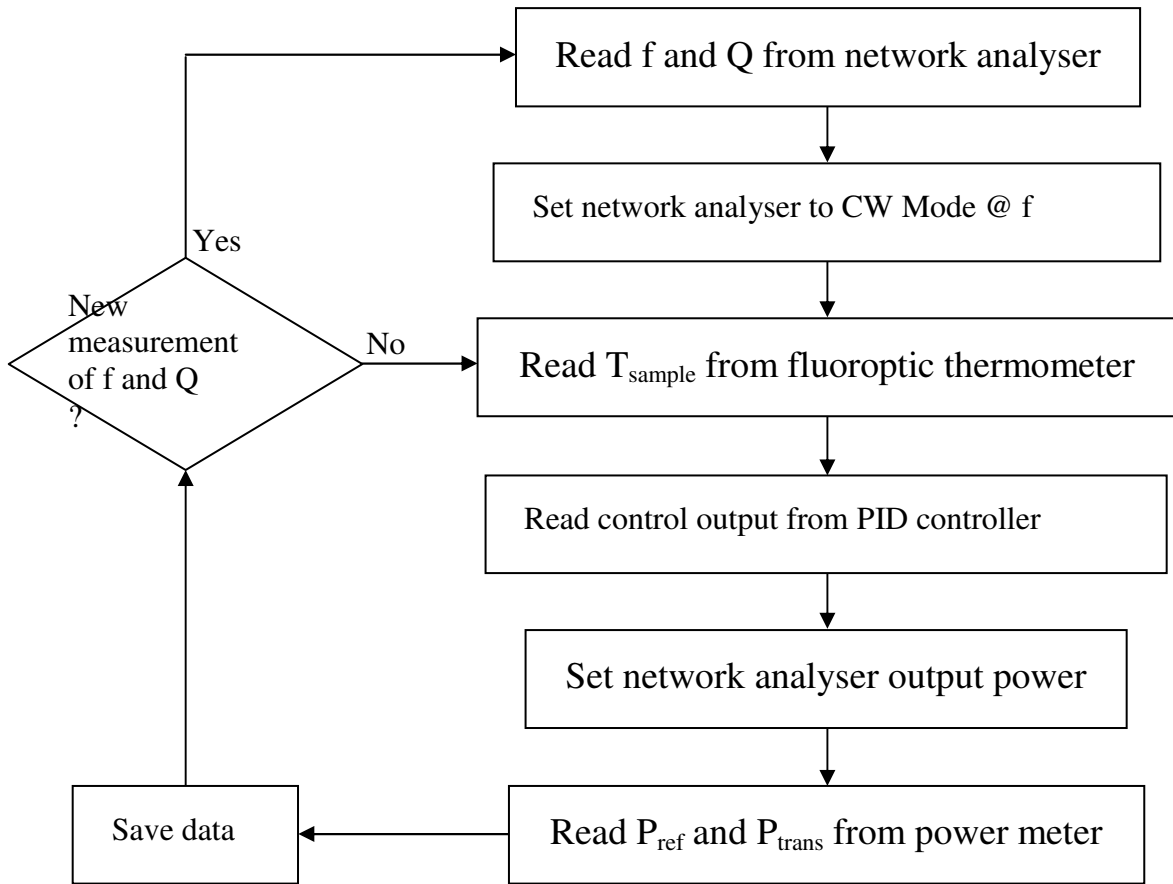


Fig. 7(a+b).

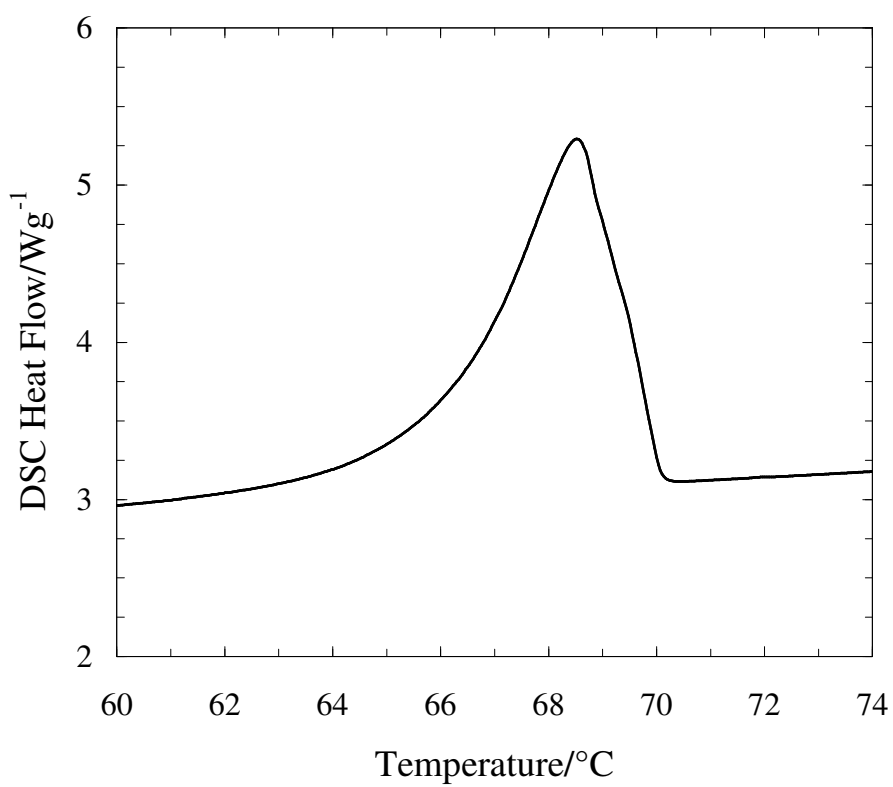
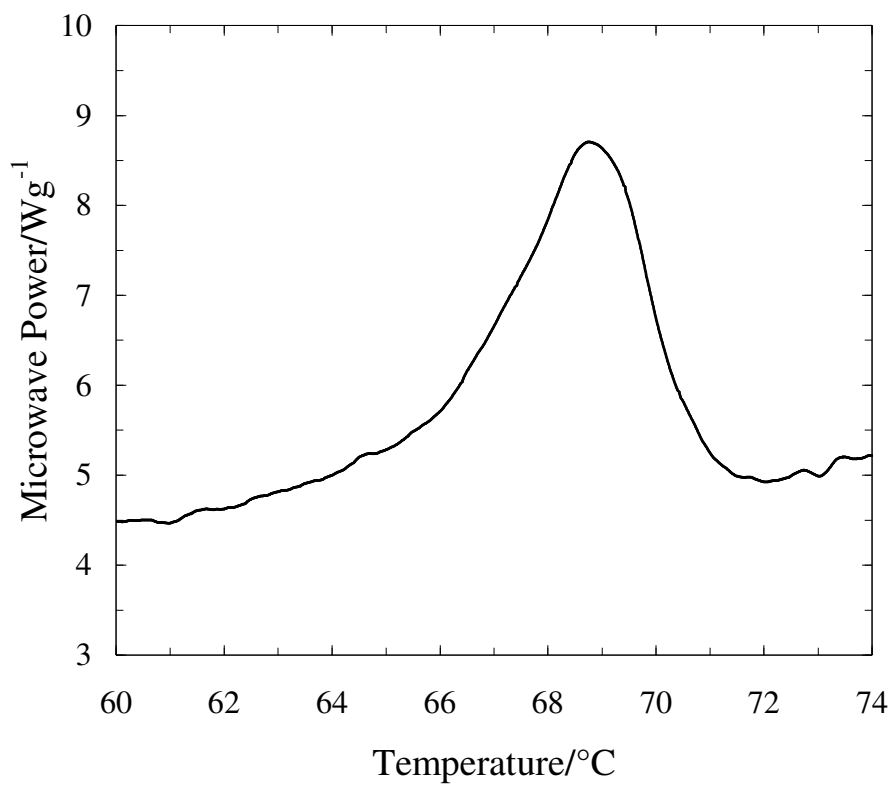


Fig. 8(a+b).

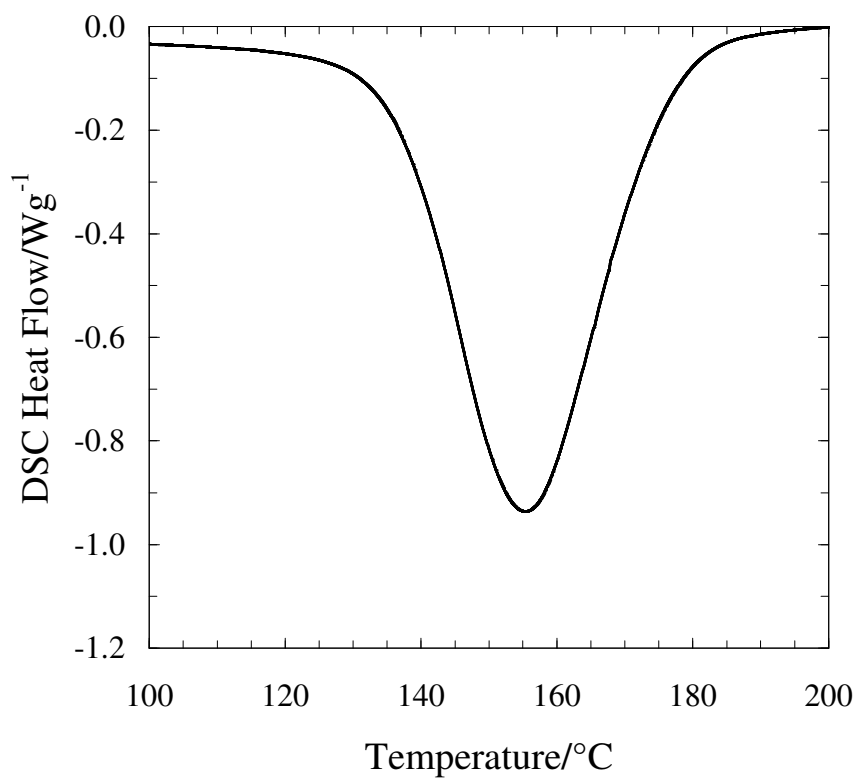
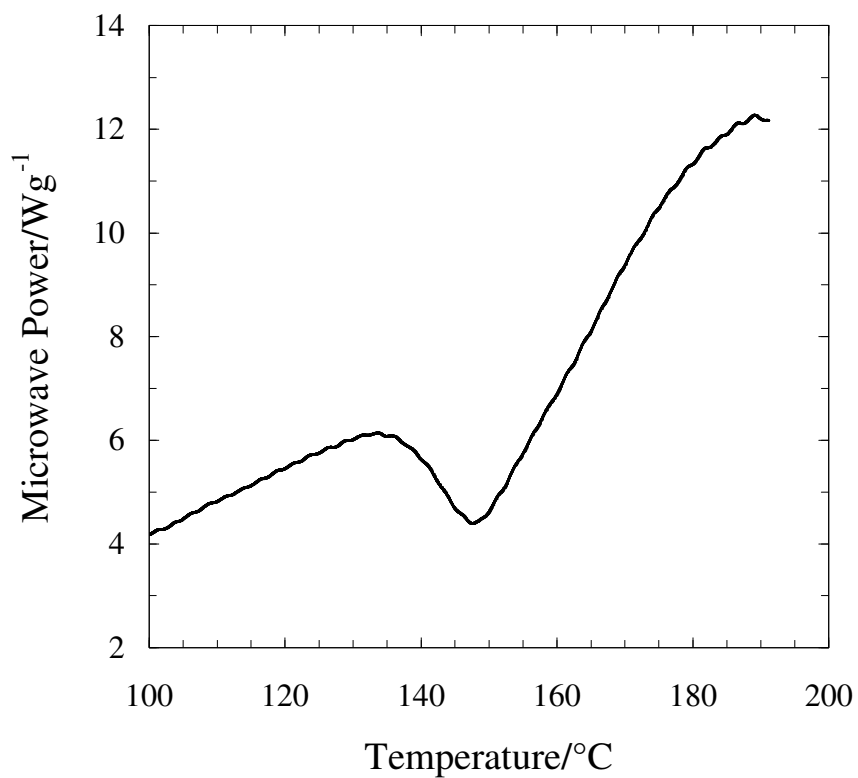


Fig. 9(a+b).

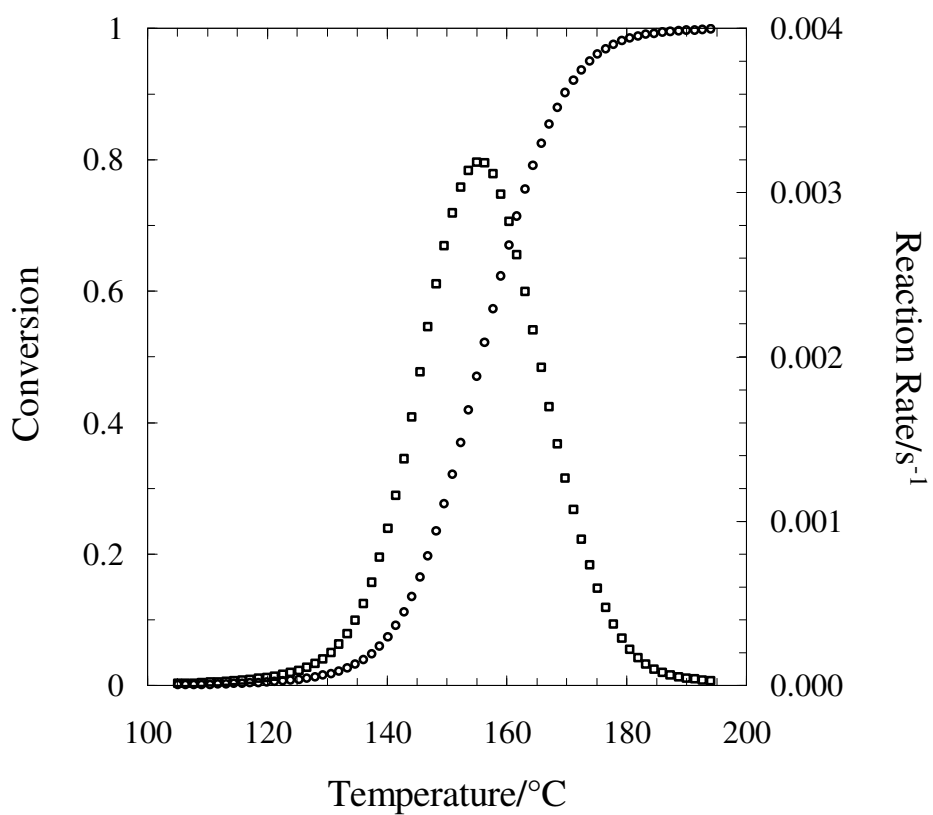
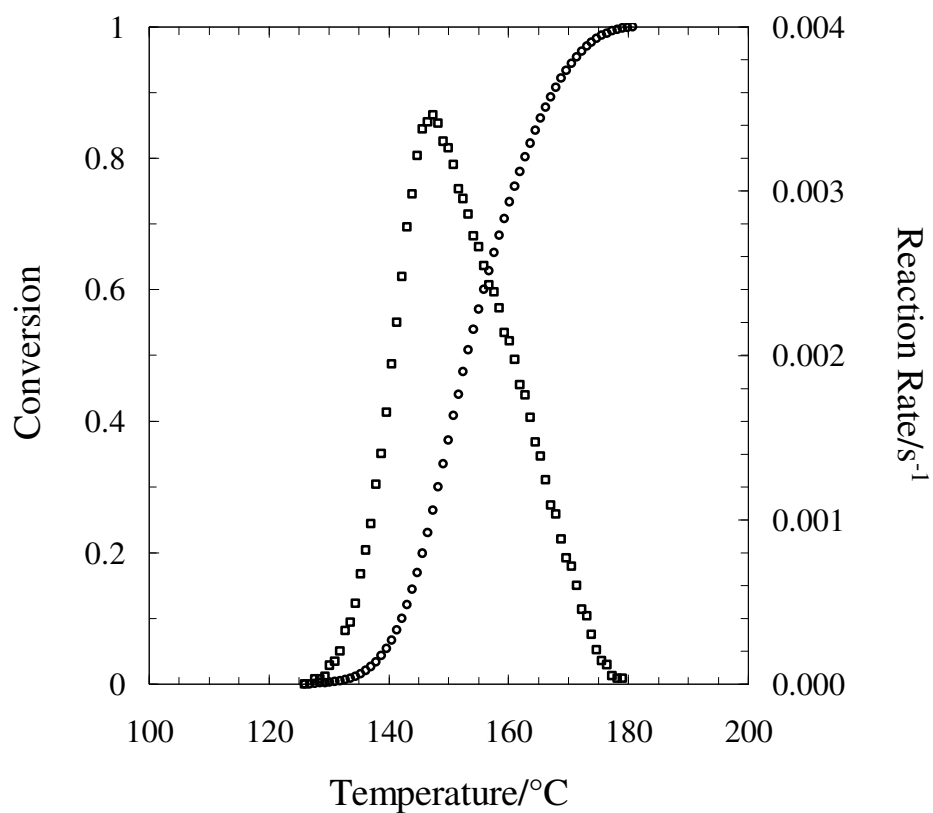


Fig. 10.

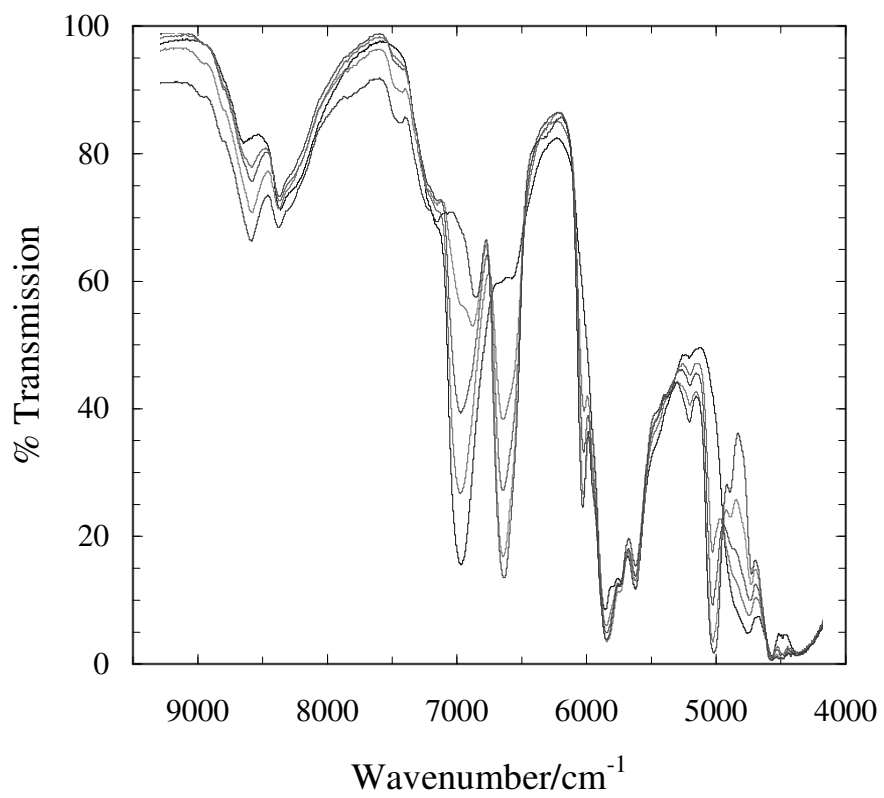


Fig. 11.

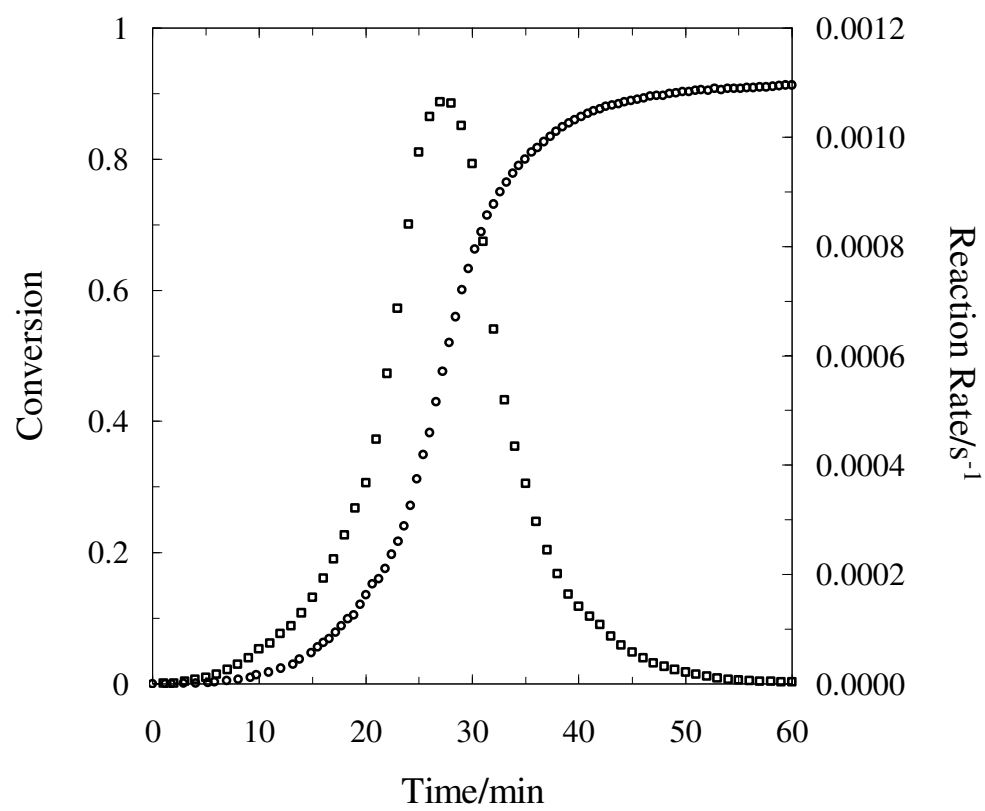


Fig. 12(a+b).

